Solitary waves, breathers, and rogue waves modulated by long waves for a model of a baroclinic shear flow

Jing-Jing Su ◉, Yi-Tian Gao,* Gao-Fu Deng, and Ting-Ting Jia

*Ministry-of-Education Key Laboratory of Fluid Mechanics and National Laboratory for Computational Fluid Dynamics,
Beijing University of Aeronautics and Astronautics, Beijing 100191, China*

Investigated in this paper is a quasigeostrophic two-layer model for the wave packets in a marginally stable or unstable baroclinic shear flow. We find that the wave packets can be modulated by certain long waves, resulting in different behaviors from those in the existing literature. Via the bilinear method, we construct the modulated Nth-order ($N = 1, 2, \ldots$) solitary waves, breathers, and rogue waves for the wave-packet equations. Based on the modulation effects of the long waves, the solitary waves are classified into three types, i.e., Type-I, Type-II, and Type-III solitary waves. Type-I solitary waves, without the modulations, are the bell shaped and propagate with constant velocities; Type-II solitary waves, with the weak modulations, are shape changing within a short time and subsequently return to the bell-shaped state; and Type-III solitary waves, with the strong modulations, show not only the variations of shapes but also the appearances, splits, combinations, and disappearances of certain bulges in the evolution. For the interaction between the two unmodulated solitary waves, two Type-I solitary waves can bring about the oscillations in the interaction zone when they possess different velocities, and bring into being the bound-state, oscillation-state, and bi-oscillation-state solitary waves when they possess the same velocity. For the two interactive modulated solitary waves, bound-state, oscillation-state, and bi-oscillation-state solitary waves with the short-time variations of shapes or appearances of bulges can occur. Due to the modulations of the long waves, breathers and rogue waves are distorted and stretched, mainly in two aspects: one is the evolution trajectories for the breathers; the other is the shape variations for each element of the breathers and rogue waves. Numbers of the peaks and valleys for the rogue waves are adjustable via the modulations. In addition, modulated breathers and rogue waves can degenerate into the M- or W-shaped or multipeak solitary waves under certain conditions.

I. INTRODUCTION

The quasigeostrophic two-layer model has been proposed to describe the nonlinear evolution of wave packets in a marginally stable or unstable baroclinic shear flow [1–7], as described in Fig. 1. In that model, two layers of the immiscible inviscid fluids, confined by rigid frictionless walls to an infinite straight channel of finite depth and width, have been presented to rotate around the vertical axis with a certain angular velocity [1–3]. Researchers have found that the denser fluid underlies the lighter to match the system's gravitational stability [1–3]. Once an equilibrium state of the system is maintained, the interface between the two layers has deviated from the original location and some gravitational potential energy has been available to be transformed into the kinetic energy of the fluid motions [1–3]. If the small disturbances in the flow can grow at the expense of the available potential energy, the fluids have been said to be baroclinically unstable, in which the infinitesimal wavelike disturbances can be expected to grow [3]. To study the evolution of such waves as their amplitudes become finite, experiments have been conducted,

demonstrating that the nonlinearities can produce more or less regular variations of the waves in time and space under a wide range of conditions [3,8–10]. Theoretically, people have supposed that the fluids flow in the form of a perturbed basic zonal shear flow, so that the asymptotic expansions of the perturbation stream functions have been used to derive the wave-packet equations [2,3]. When the Rossby number is small and the central wave number is $\sqrt{2}F$, the governing equations have been presented as [2,3,11–21]

$$\left(\frac{\partial}{\partial T} + C_{g1}\frac{\partial}{\partial X}\right)\left(\frac{\partial}{\partial T} + C_{g2}\frac{\partial}{\partial X}\right)A = \sigma^2 A - PAB,$$

$$\left(\frac{\partial}{\partial T} + C_{g2}\frac{\partial}{\partial X}\right)B = \left(\frac{\partial}{\partial T} + C_{g1}\frac{\partial}{\partial X}\right)|A|^2, \quad (1)$$

with

$$\sigma^2 = \frac{\Delta}{2|\Delta|}\ell^2\gamma^2\frac{\beta}{F}, \quad P = \frac{(m\pi\ell\gamma)^2}{4},$$

subject to the boundary condition

$$A(X, T) \to 0 \quad \text{as} \quad |X| \to \infty, \quad (2)$$

where F denotes the internal rotational Froude number, X and T denote the slowly varying along-channel and time

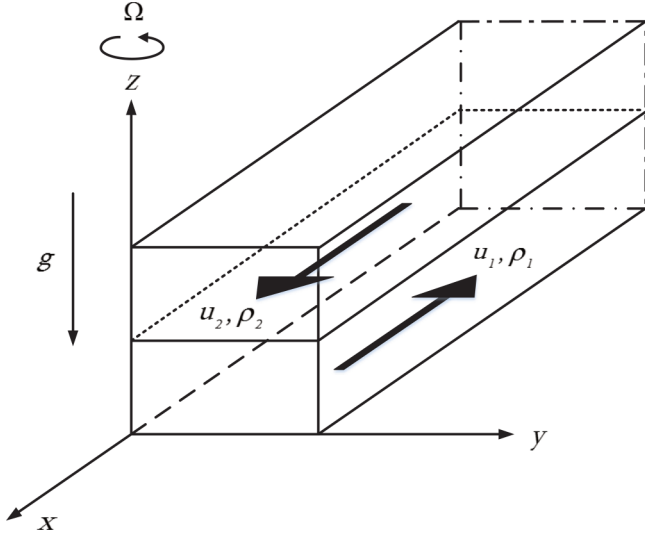*Corresponding author: gaoyt163@163.com

FIG. 1. The model proposed in Ref. [1]. Two layers of the immiscible inviscid fluids flow along an infinite straight channel with relative motion, rotating around a vertical axis with an angular velocity Ω, where x, y, and z denote the along-channel, across-channel, and vertical coordinates, respectively, u_2 and u_1 are the along-channel velocities of the upper-layer and lower-layer fluids, ρ_2 and ρ_1 are the densities of the upper-layer and lower-layer fluids, and g denotes the vertical gravitational acceleration.

coordinates, $A = A(X, T)$ is a complex function denoting the slowly varying amplitude of a baroclinic wave train in the upper layer, γ denotes the ratio of the wave amplitude of the lower layer to that of the upper layer, $B = B(X, T)$ is a real function denoting the wave-induced modification of the basic flow by the baroclinic waves,[1] C_{g1} and C_{g2} ($C_{g1} > C_{g2}$) are the group velocities of the two wave modes described by the lowest-order linear equations in the asymptotic expansions, Δ is a shear increment above the minimum critical shear $\frac{\beta}{F}$ (required for the baroclinic instability) between the two layers, β is the planetary vorticity factor, $\Delta < 0$ and $\Delta > 0$ denote the so-called subcritical and supercritical cases, respectively, π is the circular constant, ℓ is a real constant, and m is an integer [2,3]. Especially, Eqs. (1) have been reduced into the sine-Gordon equation for the real amplitude and self-induced transparency equations of nonlinear optics for the complex

---

[1]The governing wave-packet equations have been constructed based on the assumptions of the basic zonal shear flows. Placing the wave packet perturbations on the basic zonal shear flows, with the help of the multiscale method, Refs. [1,2] have derived the propagation equations for the wave packets, in which B is related to the second-order components of the perturbation stream functions in the asymptotic expansions. The first-order components (main components) of the perturbation stream functions are determined by A [1,2]. Under this circumstance, whether in the stability analyses or solution explorations of the propagation equations, B affects the amplitudes of the wave packets greatly, and thereby affects the wave packet perturbations on the basic flows [1,2].

amplitude [3]. Through the variable transformations [11–21]

$$A = \psi_1, \quad B = \frac{(C_{g1} - C_{g2})^2}{C_{g2}P}\psi_2, \quad \xi = X - C_{g1}T,$$

$$\tau = T - \frac{X}{C_{g2}}, \tag{3}$$

Eqs. (1) have been rewritten as [11–21]

$$\frac{\partial^2 \psi_1}{\partial \xi \partial \tau} = \delta \psi_1 - \psi_1 \psi_2,$$

$$\frac{\partial \psi_2}{\partial \xi} = \varsigma \frac{\partial |\psi_1|^2}{\partial \tau}, \tag{4}$$

with

$$\delta = \frac{\sigma^2 C_{g2}}{(C_{g1} - C_{g2})^2}, \quad \varsigma = \frac{P}{(C_{g1} - C_{g2})^2}, \tag{5}$$

subject to the boundary conditions

$$\psi_1 \to 0 \quad \text{as} \quad |\xi| \to \infty,$$

$$\psi_2 \to 0 \quad \text{as} \quad |\xi| \to \infty. \tag{6}$$

It has been revealed that the baroclinic wave packets can propagate in the forms of the solitary waves (solitons), breathers, rogue waves, and periodic waves [2,3,11–21]. Based on Eqs. (4), the high-order solitary wave solutions of Eqs. (1) have been obtained via the inverse scattering transformation,[2] bilinear method,[3] Darboux transformation (DT),[4] and Kadomtsev-Petviashvili hierarchy reduction[5] [2,3,11–13]. Through the DT and generalized DT, the breather and rogue wave solutions of Eqs. (1) have been derived [14–17]. Integration method has been used to derive the periodic wave solutions of Eqs. (1) [18,19]. More on analytic solutions of Eqs. (1) can be seen, e.g., in Refs. [20,21]. Solitary waves have been discovered in a narrow channel due to the invariant amplitudes and velocities in the propagation, and recognized via the Korteweg–de Vries equation for the shallow-water

---

[2]The inverse scattering transformation is known as an extension of the Fourier transform technique in the nonlinear science, which is composed of three procedures: (1) mapping of the initial data into the scattering space; (2) evolution of the scattering data over time; and (3) reconstruction of the solution of the original equation by mapping back into the physical space [3,22,23].

[3]The bilinear method is a direct approach to solve certain nonlinear evolution equations, at the heart of which lies the idea that we simplify the original equation by constructing a series of compatible subequations and solve those subequations through the small parameter expansion or method of the undetermined coefficients [24].

[4]The DT is known as a set of the recurrence formulas that connect certain seed solutions and new solutions of a nonlinear evolution equation based on a series of different spectral parameters, while in the generalized DT the spectral parameter remains the same in each iteration [25].

[5]The Kadomtsev-Petviashvili hierarchy reduction is a method to solve the nonlinear evolution equations through dividing the original equations into some separate parts and comparing those parts to the so-called Kadomtsev-Petviashvili hierarchy, the solutions of which are known [26].

waves [22,23]. In fact, people have observed that the solitary waves can propagate steadily in optical fibers, plasmas, water tanks, etc., arising from the balance between nonlinear and dispersive effects [27–33]. Rogue waves, approaching without a trace and leaving without a shadow, have captured the researchers' attention since they have caused some catastrophes for ships and offshore oil platforms [34–45]. Rogue waves have also been discovered in optics, astrophysics, fluid dynamics, and other fields [28–30].

In this paper, we will observe that the introduction of certain long waves into the wave-induced modification of basic flow brings the wave packets more diversified features. Based on those observations, this paper will be organized as follows. In Sec. II, we will introduce a long wave into the wave-induced modification of the basic flow to investigate the solitary wave mode of the baroclinic wave packets. In Sec. III, with the long wave, breather and rogue wave modes of the wave packets will be studied. Our conclusions will be presented in Sec. IV.

II. SOLITARY WAVE MODE OF THE BAROCLINIC WAVE PACKETS

A. Bilinear forms of Eqs. (4)

With the transformations

$$\psi_1 = \frac{g}{f}, \quad \psi_2 = 2\frac{\partial^2 \ln f}{\partial \xi \partial \tau} + \alpha(\tau), \tag{7}$$

we obtain the bilinear forms for Eqs. (4) as

$$
\begin{aligned}
D_\xi D_\tau f \cdot g - [\delta - \alpha(\tau)]fg &= 0, \\
D_\xi^2 f \cdot f + \varpi f^2 - \varsigma g g^* &= 0,
\end{aligned}
\tag{8}
$$

where $\alpha(\tau)$ is a real differentiable function, $g = g(\xi, \tau)$ is a complex function of ξ and τ, while $f = f(\xi, \tau)$ is a real one, ϖ is a real constant, "∗" denotes the complex conjugate, and D_ξ and D_τ are the bilinear operators defined by [24]

$$D_\xi^{n_1} D_\tau^{n_2} v_1 \cdot v_2 = \left(\frac{\partial}{\partial \xi} - \frac{\partial}{\partial \xi'}\right)^{n_1} \left(\frac{\partial}{\partial \tau} - \frac{\partial}{\partial \tau'}\right)^{n_2} v_1(\xi, \tau)v_2(\xi', \tau')\bigg|_{\xi'=\xi, \tau'=\tau}, \quad (n_1, n_2 = 0, 1, 2, \ldots),$$

with $v_1(\xi, \tau)$ being an analytic function of ξ and τ, and $v_2(\xi', \tau')$ being an analytic function of the formal variables ξ' and τ'.

B. Solitary waves of Eqs. (1)

With the help of bilinear forms (8) and the method of perturbation expansions, we derive the Nth-order solitary waves of Eqs. (4) as

$$\psi_1 = \frac{\sum_{j=1}^N g_{2j-1}}{1 + \sum_{j=1}^N f_{2j}}, \quad \psi_2 = 2\frac{\partial^2 \ln\left(1 + \sum_{j=1}^N f_{2j}\right)}{\partial \xi \partial \tau} + \alpha(\tau), \tag{9}$$

where

$$g_{2j-1} = \begin{cases} \sum_{\chi=1}^N \exp(\Xi_\chi), & (j = 1), \\ \left(\frac{\varsigma}{2}\right)^{j-1} \sum_{\Gamma_j, \Gamma'_{j-1}} \Theta_{\Gamma_1, \Gamma_2, \cdots, \Gamma_j, \Gamma'_1, \Gamma'_2, \cdots, \Gamma'_{j-1}} \exp\left[\Xi_{\Gamma_j} + \sum_{\chi=1}^{j-1}\left(\Xi_{\Gamma_\chi} + \Xi^*_{\Gamma'_\chi - N}\right)\right], & (j = 2, 3, \ldots, N), \end{cases}$$

$$f_{2j} = \left(\frac{\varsigma}{2}\right)^j \sum_{\Gamma_j, \Gamma'_j} \Theta_{\Gamma_1, \Gamma_2, \cdots, \Gamma_j, \Gamma'_1, \Gamma'_2, \cdots, \Gamma'_j} \exp\left[\sum_{\chi=1}^j \left(\Xi_{\Gamma_\chi} + \Xi^*_{\Gamma'_\chi - N}\right)\right], \quad (j = 1, 2, \ldots N),$$

with

$$\Theta_{\Gamma_1, \Gamma_2, \cdots, \Gamma_j, \Gamma'_1, \Gamma'_2, \cdots, \Gamma'_{j-1}} = \frac{\prod_{1 \leqslant \iota < J \leqslant j}\left(k_{\Gamma_\iota} - k_{\Gamma_J}\right)^2 \prod_{1 \leqslant \iota < J \leqslant j-1}\left(k^*_{\Gamma'_\iota - N} - k^*_{\Gamma'_J - N}\right)^2}{\prod_{\substack{1 \leqslant \iota \leqslant j \\ 1 \leqslant J \leqslant j-1}}\left(k_{\Gamma_\iota} + k^*_{\Gamma'_J - N}\right)^2},$$

$$\Theta_{\Gamma_1, \Gamma_2, \cdots, \Gamma_j, \Gamma'_1, \Gamma'_2, \cdots, \Gamma'_j} = \frac{\prod_{1 \leqslant \iota < J \leqslant j}\left(k_{\Gamma_\iota} - k_{\Gamma_J}\right)^2 \left(k^*_{\Gamma'_\iota - N} - k^*_{\Gamma'_J - N}\right)^2}{\prod_{1 \leqslant \iota, J \leqslant j}\left(k_{\Gamma_\iota} + k^*_{\Gamma'_J - N}\right)^2},$$

$$\Xi_\chi = k_\chi \xi + \frac{1}{k_\chi} \int [\delta - \alpha(\tau)]d\tau + \varrho_\chi, \quad \varpi = 0,$$

where Γ_ι's $(1 \leqslant \Gamma_\iota \leqslant N)$ and Γ'_j's $(N < \Gamma'_j \leqslant 2N)$ are the strictly monotone increasing positive-integer sequences with respect to their subscripts ι and J $(\iota, J = 1, 2, \ldots, j)$, k_χ's and ϱ_χ's are all the nonzero complex constants, while

$\sum_{\Gamma_j, \Gamma'_{j-1}} (\bullet)$ and $\sum_{\Gamma_j, \Gamma'_j} (\bullet)$ indicate the sums going through all the possibilities of $\bullet$. Furthermore, taking boundary condition (6) into consideration, we need $\alpha(\tau) \to 0$ as $\tau \to \infty$. Based on the above results, substitutions of expressions (3)

and (5) into Eqs. (9) yield the Nth-order solitary waves of Eqs. (1). It is noticed that when $\alpha(\tau) \equiv 0$ the solitary waves have been obtained in Refs. [2,3,11–13].

To study the effects of $\alpha(\tau)$ on the behaviors of the solitary waves, we consider $N = 1$ first. Setting $\varphi(\tau) = \int \alpha(\tau) d\tau$, we simplify the amplitudes of the first-order solitary waves for Eqs. (1) as

$$|A| = \frac{\sqrt{2}|\text{Re}(k_1)||C_{g_1} - C_{g_2}|}{\sqrt{P}} \text{sech}(\Psi),$$

$$B = \frac{2\text{Re}^2(k_1)\left[\sigma^2 C_{g2} - (C_{g1} - C_{g2})^2 \alpha\left(T - C_{g_2}^{-1}X\right)\right]}{P|k_1|^2 C_{g2}} \text{sech}^2(\Psi)$$

$$+ \frac{(C_{g1} - C_{g2})^2 \alpha\left(T - C_{g_2}^{-1}X\right)}{PC_{g2}}, \quad (10)$$

with

$$\Psi = \kappa X + \omega T - \frac{\text{Re}(k_1)}{|k_1|^2}\varphi\left(T - C_{g_2}^{-1}X\right)$$

$$+ \ln \frac{\sqrt{P}}{2\sqrt{2}\text{Re}(k_1)|C_{g_1} - C_{g_2}|} + \text{Re}(\varrho_1),$$

$$\kappa = \text{Re}(k_1)\left(1 - \frac{\sigma^2}{|k_1|^2(C_{g1} - C_{g2})^2}\right),$$

$$\omega = -\text{Re}(k_1)C_{g2}\left(\frac{C_{g1}}{C_{g2}} - \frac{\sigma^2}{|k_1|^2(C_{g1} - C_{g2})^2}\right),$$

where $\text{Re}(\bullet)$ denotes the real part of the element $\bullet$. Thus, the characteristic-line equations and propagation velocities of the solitary waves are given by

$$\kappa X + \omega T - \frac{\text{Re}(k_1)}{|k_1|^2}\varphi\left(T - C_{g_2}^{-1}X\right)$$

$$+ \ln \frac{\sqrt{P}}{2\sqrt{2}\text{Re}(k_1)|C_{g_1} - C_{g_2}|} + \text{Re}(\varrho_1) = 0, \quad (11\text{a})$$

$$v = \frac{C_{g2}\{(C_{g1} - C_{g2})^2\left[|k_1|^2 C_{g1} + \alpha\left(T - C_{g_2}^{-1}X\right)\right] - \sigma^2 C_{g2}\}}{(C_{g1} - C_{g2})^2\left[|k_1|^2 C_{g2} + \alpha\left(T - C_{g_2}^{-1}X\right)\right] - \sigma^2 C_{g2}}. \quad (11\text{b})$$

Note that X and T in Eq. (11b) are restricted by Eq. (11a). From expressions (10) and (11), we find that when $\alpha(\tau) \equiv 0$ the wave packets and wave-induced modifications of the basic flow both show as the regular bell-shaped solitary waves with the constant velocities and permanent shapes, as described in Fig. 2. When $\alpha(\tau) \not\equiv 0$, variations of the shapes and velocities of the solitary waves would occur during the propagation of the wave packets, and the modifications of the basic flow evolve in the forms of the distorted bell-shaped solitary waves with background waves, as seen in Figs. 3 and 4. In fact, the background waves are the long waves,[6] which are described by $\frac{(C_{g1} - C_{g2})^2 \alpha(T - C_{g_2}^{-1}X)}{PC_{g2}}$. In conclusion, introducing the long

---

[6]Long waves have been introduced in the wireless communications first, which can travel the distance up to 17 000 kilometers [46]. Researchers have used the long waves to describe some nonlinear phenomena characterized by the long-distance transmission [46].
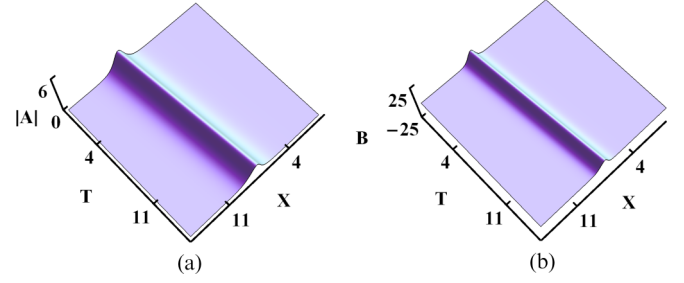

FIG. 2. Type-I solitary waves via solutions (10), with $k_1 = 2 + 3i\,(i = \sqrt{-1})$, $\varrho_1 = 0$, $\sigma = 5$, $P = C_{g2} = 1$, $C_{g1} = 2$, $\varphi(\tau) = -120$.

waves into the wave-induced modifications of the basic flow brings into being the distorted bell-shaped solitary waves for the wave packets. Those phenomena can be regarded as the modulations of the long waves to the bell-shaped solitary waves [47], where the behaviors of the long waves can be adjusted by $\alpha(\tau)$. Due to the modulations of certain long waves, Figs. 3 and 4 present two modulation behaviors of the wave packets. Considering the modulation effects of $\alpha(\tau)$ on the behaviors of the solitary waves, we classify the solitary waves into three types.

1. Type I—Solitary waves without the modulations: $\alpha(\tau) \equiv 0$

In this case, $\varphi(\tau)$ degenerates into a constant and we set it as M. As discussed above, without the modulations of the long waves, the wave packets are bell shaped and propagate with the constant velocities. We reduce the amplitudes and velocities of the solitary waves into

$$|A| = \frac{\sqrt{2}|\text{Re}(k_1)||C_{g_1} - C_{g_2}|}{\sqrt{P}} \text{sech}(\Psi),$$

$$B = \frac{2[\text{Re}(k_1)]^2\sigma^2}{P|k_1|^2} \text{sech}^2(\Psi), \quad (12)$$

$$v = \frac{|k_1|^2 C_{g1}(C_{g1} - C_{g2})^2 - \sigma^2 C_{g2}}{|k_1|^2(C_{g1} - C_{g2})^2 - \sigma^2},$$

with

$$\Psi = \kappa X + \omega T - \frac{\text{Re}(k_1)M}{|k_1|^2}$$

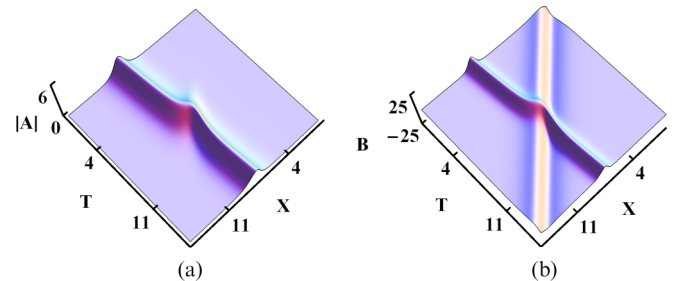$$+ \ln \frac{\sqrt{P}}{2\sqrt{2}\text{Re}(k_1)|C_{g_1} - C_{g_2}|} + \text{Re}(\varrho_1). \quad (13)$$

FIG. 3. Type-II solitary waves via solutions (10), with $k_1 = 2 + 3i$, $\varrho_1 = 0$, $\sigma = 5$, $P = C_{g2} = 1$, $C_{g1} = 2$, $\varphi(\tau) = 10\,\text{sech}(\tau) - 120$.
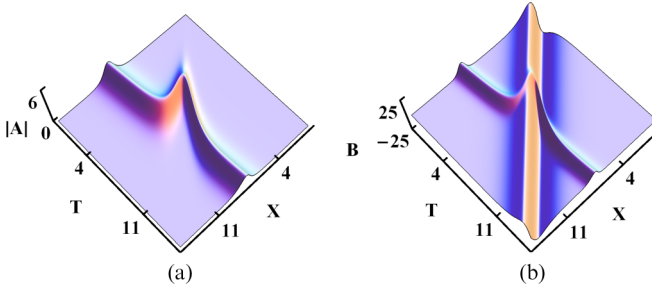
FIG. 4. Type-III solitary waves via solutions (10), with $k_1 = 2 + 3i$, $\varrho_1 = 0$, $\sigma = 5$, $P = C_{g2} = 1$, $C_{g1} = 2$, $\varphi(\tau) = 40 \operatorname{sech}(\tau) - 120$.

It is noticed that when $|k_1| = \frac{|\sigma|}{|C_{g1} - C_{g2}|}$ the solitary waves degenerate into the infinitely long plane waves. Supposing that A_0 and V are, respectively, the initial maximum amplitude and initial velocity of a wave packet, and that without loss of generality A_0 is restricted to a positive number, we have

$$\operatorname{Re}(k_1) = \frac{\sqrt{P} A_0}{\sqrt{2}(C_{g_1} - C_{g_2})}, \quad |k_1|^2 = \frac{\sigma^2 (V - C_{g2})}{(C_{g1} - C_{g2})^2 (V - C_{g1})},$$
(14)

so that

$$\frac{P A_0^2}{2} \leqslant \frac{\sigma^2 (V - C_{g2})}{(V - C_{g1})}.$$
(15)

When $\sigma^2 > 0$ (supercritical case), we can obtain a critical amplitude $\tilde{A}_0 = \sqrt{\frac{2\sigma^2}{P}}$ for which $|V|$ becomes infinite. If $0 < A_0 < \tilde{A}_0$, V is in the range of $(-\infty, \frac{PA_0^2 C_{g1} - 2\sigma^2 C_{g2}}{PA_0^2 - 2\sigma^2})$ or $(C_{g1}, +\infty)$. If $A_0 > \tilde{A}_0$, V is in the range of $(C_{g1}, \frac{PA_0^2 C_{g1} - 2\sigma^2 C_{g2}}{PA_0^2 - 2\sigma^2})$. No matter which range A_0 is in, $V > C_{g1}$ or $V < C_{g2}$ always holds, indicating that the propagation velocities of the wave packets lie outside the velocity interval bounded by the two group velocities. When $\sigma^2 < 0$ (subcritical case), V is in the range of $(\frac{PA_0^2 C_{g1} - 2\sigma^2 C_{g2}}{PA_0^2 - 2\sigma^2}, C_{g1})$. Compared with those in Ref. [2], the more precise ranges of the propagation velocities in the both cases are given.

2. Type II—Solitary waves with the weak modulations[7]: $\frac{\sigma^2 C_{g2} - |k_1|^2 C_{g2} (C_{g1} - C_{g2})^2}{(C_{g1} - C_{g2})^2} \notin S[\alpha(\tau)]$[8]

When the range of $\alpha(\tau)$ is so small that $\frac{\sigma^2 C_{g2} - |k_1|^2 C_{g2} (C_{g1} - C_{g2})^2}{(C_{g1} - C_{g2})^2} \notin S[\alpha(\tau)]$, short-time shape variations and subsequent restorations to the initial state occur in the propagation of the wave packets, as shown in Fig. 3. In this case, the wave packets are modulated by the amplitude-limited long waves and return to the bell state, indicating that the effects of the modulations are rather weak. Under this circumstance, we deem that the wave packets undergo the weak modulations in the evolution. It is also demonstrated that the solitary waves possess a certain degree of the nonlinear stability.

3. Type III—Solitary waves with the strong modulations: $\frac{\sigma^2 C_{g2} - |k_1|^2 C_{g2} (C_{g1} - C_{g2})^2}{(C_{g1} - C_{g2})^2} \in S[\alpha(\tau)]$

When the range of $\alpha(\tau)$ grows, i.e., $\frac{\sigma^2 C_{g2} - |k_1|^2 C_{g2} (C_{g1} - C_{g2})^2}{(C_{g1} - C_{g2})^2} \in S[\alpha(\tau)]$, indicating that the strong modulations occur in the

---

[7]Modulation is a process of adding the information of the signal source to the carrier wave to make it suitable for the channel transmission [48]. Based on the effect on the modulating signal, modulation is divided into the weak and strong modulations [48]. When the amplitude of the carrier signal is less than a critical value, modulation is called the weak modulation, and when the amplitude of the carrier signal is more than the critical value, modulation is called the strong modulation [48].

[8]$S[\alpha(\tau)]$ denotes the range of the function $\alpha(\tau)$.
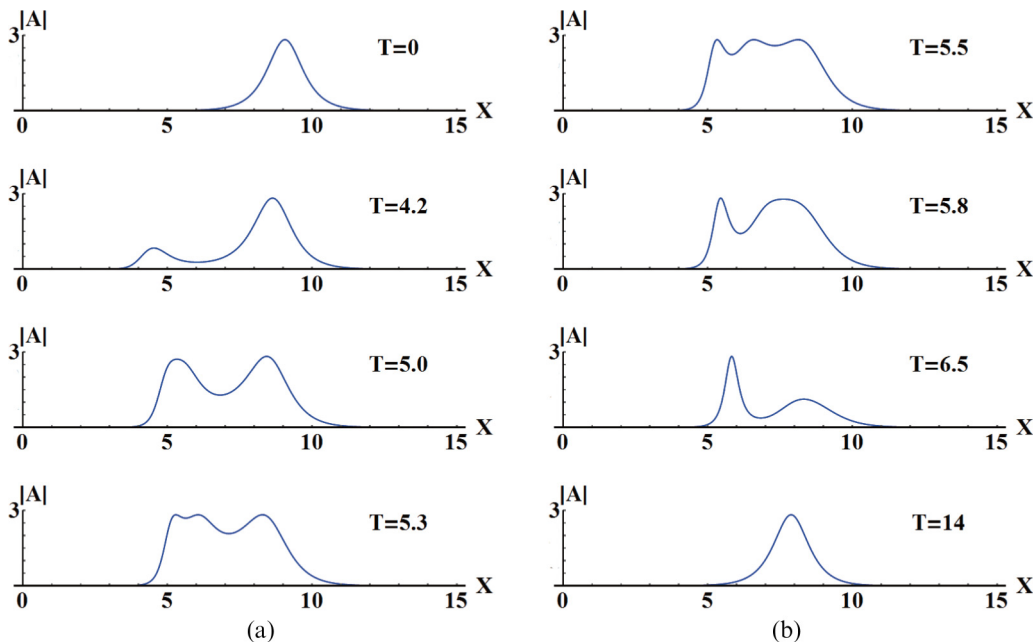

FIG. 5. Wave packet in the form of Type-III solitary waves, with the parameters the same as those in Fig. 4.
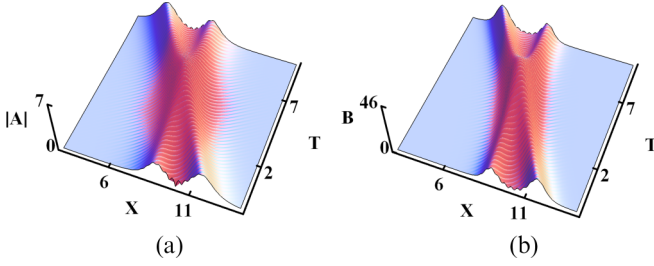
FIG. 6. Two Type-I solitary waves with oscillations in the interaction zones via solutions (9), with $k_1 = 2 - 3i$, $k_2 = \frac{5}{2} + 3i$, $\varrho_1 = \varrho_2 = 0$, $\sigma = 5$, $P = C_{g2} = 1$, $C_{g1} = 2$, $\varphi(\tau) = -120$.

evolution of the solitary waves, the wave packets show not only the variations of shapes but also the appearance of some new bulges, as seen in Fig. 4. We also illustrate the evolution of the wave packet in Fig. 5. When $T \leqslant 0$, the wave packet performs a steady solitary wave propagating forward with a constant velocity and shape. At $T = 4.2$, affected by the modulation of a long wave, the wave packet develops a bulge at the point $X = 4.5$. The bulge grows and moves until its maximum amplitude is reached at $T = 5.0$, and then it divides into two parts at $T = 5.3$. One part of the bulge moves forward and combines with that steady solitary wave into a whole, which gradually disappears at last, while the other part keeps moving with the shape changing until it possesses the same shape and velocity as the solitary wave at $T = 0$. Different from the evolution of the baroclinic waves in the above two cases, the solitary waves hereby are characterized by the appearances, splits, combinations, and disappearances of those bulges.

Note that under the condition $\text{Im}(k_1) \to \infty$ [where $\text{Im}(\bullet)$ denotes the imaginary part of the element $\bullet$], for the latter two cases, $\alpha(\tau)$ has no effect on the behaviors of the wave packets while it still affects the modifications of the basic flow, and at this point the propagation velocities of the wave packets are exactly C_{g1}.

C. Interaction between the two solitary waves of Eqs. (1)

1. Case A: Interaction between the two Type-I solitary waves of Eqs. (1)

Baroclinic wave packets can also evolve in the form of multisolitary waves. In what follows, we take the second-order solitary waves as an example to investigate the behaviors of the wave packets. Considering $\alpha(\tau) \equiv 0$ and $\varphi(\tau) = M$
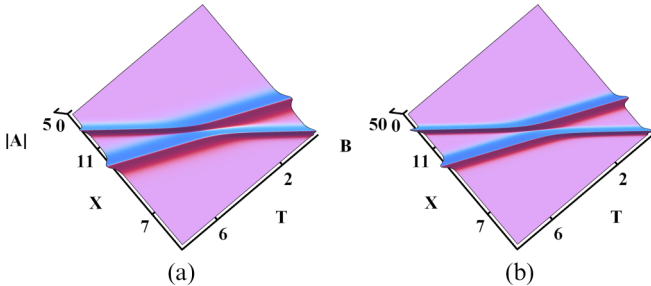

FIG. 7. Two Type-I solitary waves without oscillations in the interaction zones via solutions (9), with $k_1 = 3$, $k_2 = 2$, $\varrho_1 = \varrho_2 = 0$, $\sigma = 5$, $P = C_{g2} = 1$, $C_{g1} = 2$, $\varphi(\tau) = -120$.

first, we illustrate the evolution of the second-order solitary waves in Figs. 6 and 7. Figure 6 shows that two single solitary waves with different velocities interact with each other, bringing about the phase shifts and regular oscillations in the interaction zones. Figure 7 shows that the two interactive solitary waves propagate without the oscillations. Based on those observations, we find that under certain conditions the characteristic lines of both solitary waves are approximately the straight lines for large $|T|$. Under that circumstance, with the assumptions that the characteristic-line equations of one solitary wave before and after the interaction are, respectively, $X = v_- T + \phi_-$ and $v_+ T + \phi_+$, we have

$$\lim_{T \to +\infty} |A||_{X = v_+ T + \phi_+} = \mathcal{A}_+ \neq 0,$$
$$\lim_{T \to -\infty} |A||_{X = v_- T + \phi_-} = \mathcal{A}_- \neq 0, \tag{16}$$

where v_- (v_+) and $\mathcal{A}_-$ ($\mathcal{A}_+$) are the velocity and amplitude of the solitary wave long before (after) the interaction, while $\phi_+ - \phi_-$ is the phase shift of the solitary wave. Meanwhile, we set $k_j = a_j + b_j i$, $\varrho_j = c_j + d_j i$, where $i = \sqrt{-1}$, a_j's, b_j's, c_j's, and d_j's ($j = 1, 2$) are all the real constants, and rewrite $|A|$ as

$$|A| = \frac{|g_1 + g_3|}{|1 + f_2 + f_4|}, \tag{17}$$

where $|g_1 + g_3|$ and $|1 + f_2 + f_4|$ are presented in Appendix A. From Eq. (17), we find that $\lim_{T \to +\infty} |A||_{X = v_+ T + \phi_+} (\lim_{T \to -\infty} |A||_{X = v_- T + \phi_-})$ exists while nonzero if and only if the coefficient of H or G with respect to T under the constraint $X = v_+ T + \phi_+$ ($X = v_- T + \phi_-$) equals zero, i.e., $\Upsilon_+(\Upsilon_-) = 0$ or $\Lambda_+(\Lambda_-) = 0$, where

$$\Upsilon_\pm = v_\pm a_1 \left[1 - \frac{\sigma^2}{(a_1^2 + b_1^2)(C_{g1} - C_{g2})^2} \right]$$
$$- a_1 \left[C_{g1} - \frac{\sigma^2 C_{g2}}{(a_1^2 + b_1^2)(C_{g1} - C_{g2})^2} \right],$$

$$\Lambda_\pm = v_\pm a_2 \left[1 - \frac{\sigma^2}{(a_2^2 + b_2^2)(C_{g1} - C_{g2})^2} \right]$$
$$- a_2 \left[C_{g1} - \frac{\sigma^2 C_{g2}}{(a_2^2 + b_2^2)(C_{g1} - C_{g2})^2} \right]. \tag{18}$$

The two solutions of v_- (v_+), respectively, correspond to the velocities of the two branches of the second-order solitary waves before (after) the interaction. For $\Upsilon_\pm = 0$ or $\Lambda_\pm = 0$, we both have $v_+ = v_-$, which implies that the velocities of the two branches remain unchanged after the interaction. Hereby, we take five cases into consideration. (1) When $\Upsilon_\pm = 0$ and $\Lambda_\pm > 0$, we have

$$v_- = v_+ = \frac{(a_1^2 + b_1^2)C_{g1}(C_{g1} - C_{g2})^2 - \sigma^2 C_{g2}}{(a_1^2 + b_1^2)(C_{g1} - C_{g2})^2 - \sigma^2}, \tag{19}$$

where v_- and v_+, respectively, correspond to the velocities of one branch of the second-order solitary waves before and after the interaction. Through some mathematical operations, we derive

$$\phi_+ = \frac{(C_{g1} - C_{g2})^2}{(a_1^2 + b_1^2)(C_{g1} - C_{g2})^2 - \sigma^2}\left[M - \frac{c_1(a_1^2 + b_1^2)}{a_1} + \frac{a_1^2 + b_1^2}{2a_1}\ln\frac{8a_1^2 s_1^2(C_{g1} - C_{g2})^2}{Ps_2^2}\right],$$

$$\phi_- = \frac{(C_{g1} - C_{g2})^2}{(a_1^2 + b_1^2)(C_{g1} - C_{g2})^2 - \sigma^2}\left[M - \frac{c_1(a_1^2 + b_1^2)}{a_1} + \frac{a_1^2 + b_1^2}{2a_1}\ln\frac{8a_1^2(C_{g1} - C_{g2})^2}{P}\right],$$

$$\mathcal{A}_+ = \frac{2a_1^2(C_{g1} - C_{g2})^2}{P}, \quad \mathcal{A}_- = \frac{2a_1^2(C_{g1} - C_{g2})^2}{P}. \tag{20}$$

Subsequently, we have

$$\mathcal{A}_+ = \mathcal{A}_- = \frac{2a_1^2(C_{g1} - C_{g2})^2}{P}, \quad \phi_+ - \phi_- = \frac{(a_1^2 + b_1^2)(C_{g1} - C_{g2})^2}{a_1\left[(a_1^2 + b_1^2)(C_{g1} - C_{g2})^2 - \sigma^2\right]}\ln\frac{(a_1 + a_2)^2 + (b_1 - b_2)^2}{(a_1 - a_2)^2 + (b_1 - b_2)^2}, \tag{21}$$

which reveal that the amplitude of that branch remains unchanged after the interaction while the phase shift occurs. (2) When $\Upsilon_\pm = 0$ and $\Lambda_\pm < 0$, the same results as presented in Eqs. (21) are obtained except that the phase shift becomes the opposite. (3) When $\Upsilon_\pm > 0$ and $\Lambda_\pm = 0$, we derive the velocity, amplitude, and phase shift of the other branch of the second-order solitary waves as

$$v_\pm = \frac{(a_2^2 + b_2^2)C_{g1}(C_{g1} - C_{g2})^2 - \sigma^2 C_{g2}}{(a_2^2 + b_2^2)(C_{g1} - C_{g2})^2 - \sigma^2}, \quad \mathcal{A}_\pm = \frac{2a_2^2(C_{g1} - C_{g2})^2}{P},$$

$$\phi_+ - \phi_- = \frac{(a_2^2 + b_2^2)(C_{g1} - C_{g2})^2}{a_2\left[(a_2^2 + b_2^2)(C_{g1} - C_{g2})^2 - \sigma^2\right]}\ln\frac{(a_1 + a_2)^2 + (b_1 - b_2)^2}{(a_1 - a_2)^2 + (b_1 - b_2)^2}. \tag{22}$$

It is found that the velocity and amplitude of the other branch also remain unchanged after the interaction. (4) When $\Upsilon_\pm > 0$ and $\Lambda_\pm = 0$, the same results as expressed in Eqs. (22) are obtained except that the phase shift turns to be the opposite. In the above four cases, the interactions between the two solitary waves look like "elastic". (5) For the case $\Upsilon_\pm = 0$ and $\Lambda_\pm = 0$, $\lim_{T \to +\infty}|A|\big|_{X = v_\pm T + \phi_\pm} \neq 0$ exist if and only if $a_2 = a_1$ and $b_2 = b_1$. At this point the second-order solitary waves degenerate into the first-order solitary waves. Apart from the behaviors in the above five cases, the aforementioned two branches of the second-order solitary waves can also be characterized by the periodic variations in their own shapes and velocities, and this periodic variation characteristic becomes more visible when they become closer, where the distances between those two branches are related to c_1 and c_2, as seen in Figs. 8 and 9. In Fig. 8, the bound-state solitary waves caused by the periodic interactions of the two solitary waves are observed. Figure 9 presents an interaction in which those two branches harmonize and do not bring into the wave packet more unexpected high peaks and low valleys. Hence, the we call them oscillation-state and bi-oscillation-state solitary waves.

2. Case B: Interactions between the Type-II–Type-II, Type-II–Type-III, and Type-III–Type-III solitary waves of Eqs. (1)

For $\alpha(\tau) \not\equiv 0$, the two branches of the second-order solitary waves are both the modulated solitary waves. When $a_1^2 + b_1^2 = a_2^2 + b_2^2$, the bound-state, oscillation-state, and bi-oscillation-state solitary waves can also be observed during

the interaction of the two modulated solitary waves. As expected, two interactive Type-II solitary waves lead to the short-time variations in their shapes, while two interactive
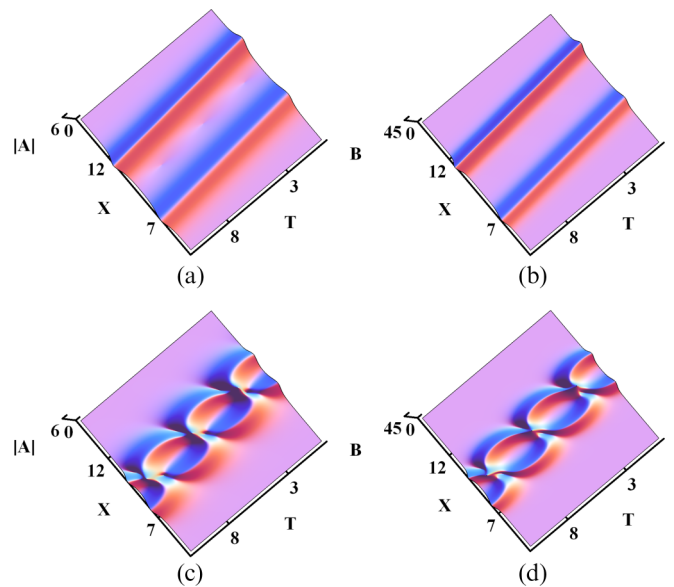

FIG. 8. Interaction between the two Type-I solitary waves brings into being the bound-state solitary waves via solutions (9), with $k_1 = \frac{5}{2} + \frac{3\sqrt{3}}{2}i$, $k_2 = -2 + 3i$, $\sigma = 5$, $P = C_{g2} = 1$, $C_{g1} = 2$, $\varphi(\tau) = -120$, $\varrho_1 = 3$, $\varrho_2 = 2$ (the first line), and $\varrho_1 = \varrho_2 = 0$ (the second line).
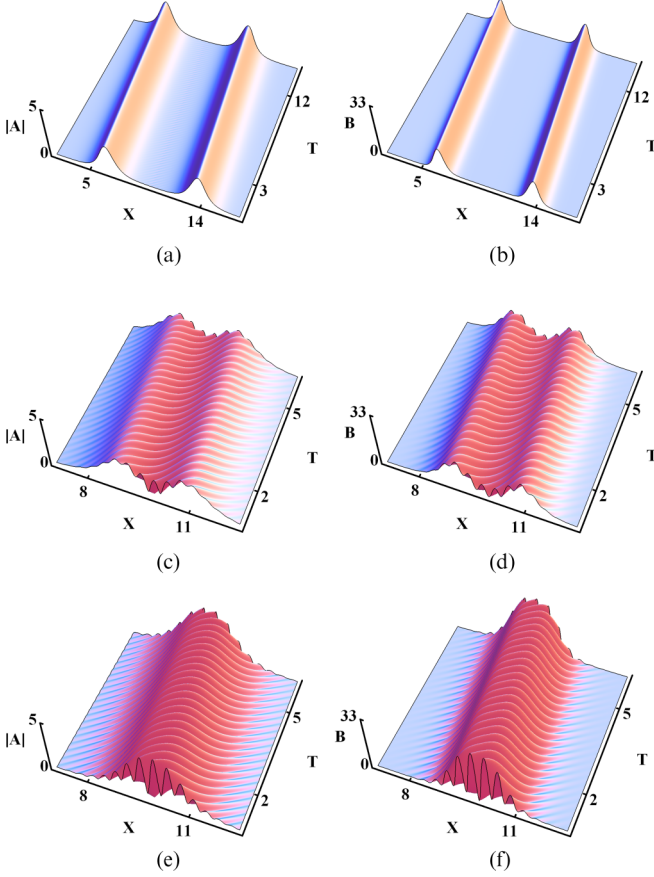
(a)　(b)　(c)　(d)　(e)　(f)

FIG. 9. Interaction between the two Type-I solitary waves brings into being the oscillation-state and bi-oscillation-state solitary waves via solutions (9), with $k_1 = 2 - 3i$, $k_2 = -2 + 3i$, $\sigma = 5$, $P = C_{g2} = 1$, $C_{g1} = 2$, $\varphi(\tau) = -120$, $\varrho_1 = \varrho_2 = -5$ (the first line), $\varrho_1 = \varrho_2 = 0$ (the second line), and $\varrho_1 = \varrho_2 = 1$ (the third line).

Type-III solitary waves lead to the appearance of the bulges, as seen in Figs. 10 and 11. Figure 12 shows that the weak oscillations may appear in the interaction zone of Type-II and Type-III solitary waves. In fact, if we set $\alpha(\tau) \equiv 0$ or reset the phase of one solitary wave in Fig. 12, Type-II and Type-III
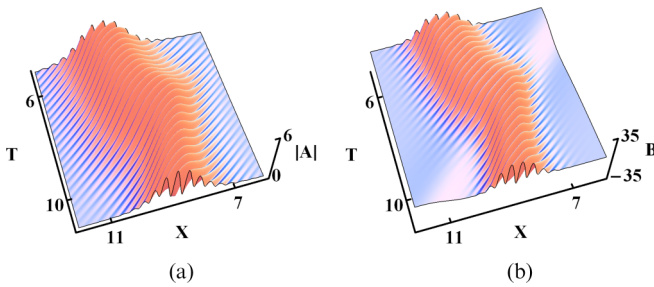

(a)　(b)

FIG. 10. Interaction between the two Type-II solitary waves via solutions (9), with $k_1 = 2 - 3i$, $k_2 = -2 + 3i$, $\varrho_1 = \varrho_2 = 1$, $\sigma = 5$, $P = C_{g2} = 1$, $C_{g1} = 2$, $\varphi(\tau) = 10 \operatorname{sech}(\tau) - 120$.
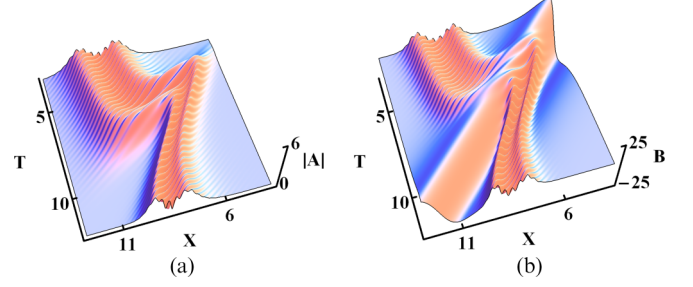

(a)　(b)

FIG. 11. Interaction between the two Type-III solitary waves via solutions (9), with $k_1 = 2 - 3i$, $k_2 = -2 + 3i$, $\varrho_1 = \varrho_2 = 0$, $\sigma = 5$, $P = C_{g2} = 1$, $C_{g1} = 2$, $\varphi(\tau) = 40 \operatorname{sech}(\tau) - 120$.

solitary waves will lead to the same oscillations as those in Fig. 6 except that the oscillations are weakened.

III. BREATHER AND ROGUE WAVE MODES OF THE BAROCLINIC WAVE PACKETS

In this section, we will investigate the modulation effects of the long waves on the breathers and rogue waves. Assuming that

$$
\begin{aligned}
g &= \lambda e^{i[Q\xi + R(\tau)]} [1 + \vartheta_1 e^{K\xi + W(\tau) + \Phi} + \vartheta_2 e^{K^*\xi + W^*(\tau) + \Phi^*} \\
&\quad + p\vartheta_1\vartheta_2 e^{(K+K^*)\xi + W(\tau) + W^*(\tau) + \Phi + \Phi^*}], \\
f &= 1 + e^{K\xi + W(\tau) + \Phi} + e^{K^*\xi + W^*(\tau) + \Phi^*} \\
&\quad + p e^{(K+K^*)\xi + W(\tau) + W^*(\tau) + \Phi + \Phi^*},
\end{aligned}
\tag{23}
$$

and substituting them in bilinear forms (8), we present ϖ, p, ϑ_1, ϑ_2, $R(\tau)$, and $W(\tau)$ in Appendix B with K ($K \neq 0$) and Φ being the complex constants, and λ and Q being the nonzero real constants. Then, the breather solutions of Eqs. (4)
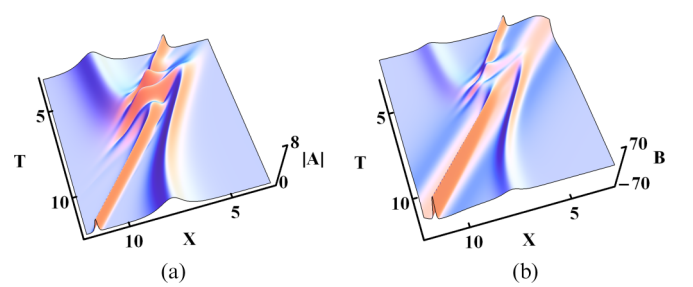

(a)　(b)

FIG. 12. Interaction between Type-II and Type-III solitary waves via solutions (9), with $k_1 = 2 - 3i$, $k_2 = -2$, $\varrho_1 = 0$, $\varrho_2 = 25$, $\sigma = 5$, $P = C_{g2} = 1$, $C_{g1} = 2$, $\varphi(\tau) = 40 \operatorname{sech}(\tau) - 120$.

are presented as

$$\psi_1 = \lambda e^{i[Q\xi + R(\tau)]} \frac{1 + \vartheta_1 e^{K\xi + W(\tau) + \Phi} + \vartheta_2 e^{K^*\xi + W^*(\tau) + \Phi^*} + p\vartheta_1\vartheta_2 e^{(K+K^*)\xi + W(\tau) + W^*(\tau) + \Phi + \Phi^*}}{1 + e^{K\xi + W(\tau) + \Phi} + e^{K^*\xi + W^*(\tau) + \Phi^*} + pe^{(K+K^*)\xi + W(\tau) + W^*(\tau) + \Phi + \Phi^*}},$$

$$\psi_2 = 2\frac{\partial^2}{\partial\xi\partial\tau}\ln[1 + e^{K\xi + W(\tau) + \Phi} + e^{K^*\xi + W^*(\tau) + \Phi^*} + pe^{(K+K^*)\xi + W(\tau) + W^*(\tau) + \Phi + \Phi^*}] + \alpha(\tau). \tag{24}$$

Setting $\Phi = i\pi$ and taking $K \to 0$, we obtain the rogue wave solutions of Eqs. (4) as

$$\begin{aligned} \psi_1 &= \lambda e^{i[Q\xi + R(\tau)]}\left(1 + \frac{\hat{g}}{\hat{f}}\right), \\ \psi_2 &= 2\frac{\partial^2 \ln\hat{f}}{\partial\xi\partial\tau} + \alpha(\tau), \end{aligned} \tag{25}$$

with

$$\begin{aligned} \hat{f} &= (Q^2 + 2\lambda^2\varsigma)(2\lambda^2\xi^2\varsigma + 1) + 2\lambda^2\varsigma R(\tau)[R(\tau) - 2Q\xi], \\ \hat{g} &= 8i\lambda^2\varsigma R(\tau) - 4(Q^2 + 2\lambda^2\varsigma). \end{aligned}$$

Substituting Eqs. (24) and (25) into Eqs. (3), respectively, we can obtain the modulated breathers and rogue waves of Eqs. (1). Due to the modulation of the long wave $\frac{(C_{g1} - C_{g2})^2}{C_{g2}P}\alpha(T - C_{g2}^{-1}X)$, evolution behaviors of the wave packets (whether in the form of the breathers or rogue waves) are enriched, as described in Figs. 13 and 14. In Refs. [14–17], the breathers without the modulations propagate with the periodic shape variations on several straight lines, and the rogue waves without the modulations possess the symmetrical structures composed of multiple peaks and valleys. Apart from those behaviors, the wave packets can also exhibit the following additional behaviors.

On the one hand, for the modulated breathers, evolution trajectories of the wave packets lose the linear property and are determined by $\alpha(\tau)$, while the modifications of the basic flow propagate with the long-wave backgrounds. Besides, each element of the breathers, which is actually a rogue wave, is distorted and stretched. Those distortions and stretches become more visible in the evolution of the modulated rogue waves. Taking the first-order rogue waves as an example, we find that the connections between the two valleys and one peak lose the original collinearity. On the other hand, modulated rogue waves exhibit more peaks and valleys on the X-T plane

than the unmodulated rogue waves, and changing $\alpha(\tau)$ we can adjust the numbers of the peaks and valleys of the rogue waves. For instance, if $\alpha(\tau)$ is selected as a linear function, via the analysis on Eqs. (25), there will be at most two peaks and four valleys on the X-T plane for the first-order rogue waves, and certainly, with the parameter regulations, we may obtain the rogue waves with one peak and three valleys. Similarly, if $\alpha(\tau)$ is a quadratic function, we will observe the first-order rogue waves with three peaks and six valleys at most. If $\alpha(\tau)$ is a sine function, we will observe the rogue waves with the innumerable peaks and valleys. Note that the maximum amplitudes of the modulated breathers and rogue waves are unrelated to $\alpha(\tau)$. In addition, under the condition $\alpha(\tau) \equiv \delta$, the breathers develop into the M- or W-shaped solitary waves or multipeak solitary waves, while the rogue waves develop into the W-shaped solitary waves, as described in Figs. 15 and 16.

IV. CONCLUSIONS

In this paper, we have investigated the quasigeostrophic two-layer model, as shown in Fig. 1, which is used to describe the nonlinear evolution of the wave packets in a marginally stable or unstable baroclinic shear flow. Introducing certain long waves into the wave-induced modifications of the basic flow, we have found that the wave packets are modulated by the long waves, resulting in different behaviors from those in Refs. [2,3,11–21]. With the bilinear method, modulated Nth-order solitary waves (9), breathers (24), and rogue waves (25) for wave-packet equations (1) have been constructed. Based on the modulation effects of the long waves, the solitary waves have been classified into three types: Type-I, Type-II, and Type-III solitary waves, as described in Figs. 2–5. It has been found that Type-I solitary waves, without the modulations, propagate with the constant velocities and permanent bell shapes; that Type-II solitary waves, with the weak modulations, are shape changing within a short time and
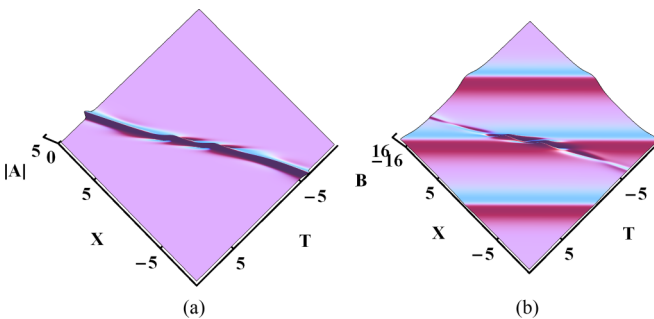

(a)   (b)

FIG. 13. Breathers via solutions (24), with $P = C_{g2} = Q = \sigma = \lambda = 1$, $C_{g1} = K = 2$, $\Phi = 0$, $\alpha(\tau) = 10\operatorname{sech}(\tau) + 10\operatorname{sech}(\tau + 10) + 10\operatorname{sech}(\tau - 10)$.
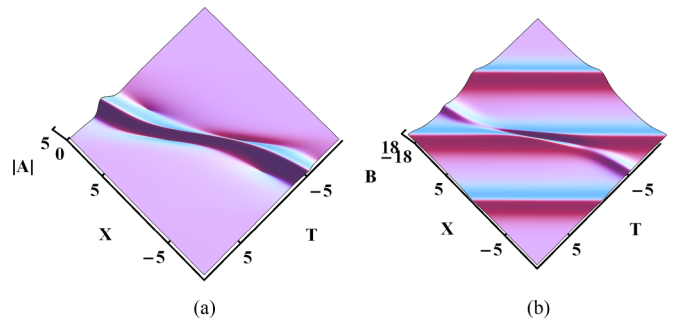

(a)   (b)

FIG. 14. Rogue waves via solutions (25), with $P = \frac{1}{5}$, $C_{g2} = Q = \sigma = \lambda = 1$, $C_{g1} = 2$, $\alpha(\tau) = 3\operatorname{sech}(\tau) + 3\operatorname{sech}(\tau + 10) + 3\operatorname{sech}(\tau - 10)$.
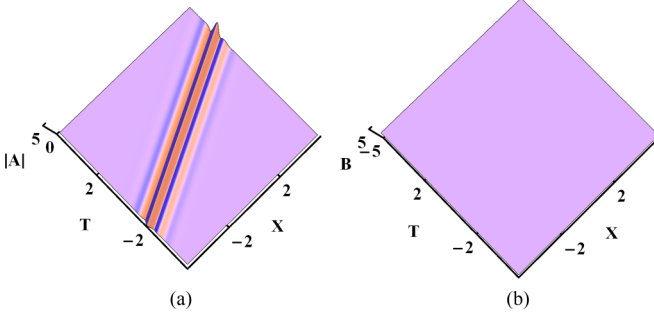
FIG. 15. Multipeak solitary waves via solutions (25), with $P = C_{g2} = Q = \sigma = \lambda = 1$, $C_{g1} = 2$, $K = 2 + 3i$, $\Phi = 0$, $\alpha(\tau) = 1$.

FIG. 16. W-shaped solitary waves via solutions (25), with $P = \frac{1}{5}$, $C_{g2} = Q = \sigma = \lambda = 1$, $C_{g1} = 2$, $\alpha(\tau) = 1$.

subsequently return to the bell-shaped state; and that Type-III solitary waves, with the strong modulations, propagate with not only the shape variations but also the appearances, splits, combinations, and disappearances of certain bulges. For the interaction between the two unmodulated solitary waves, it has been revealed that the two Type-I solitary waves with different velocities can bring about the oscillations in the interaction zone, as described in Figs. 6 and 7, and that the two Type-I solitary waves with the same velocity bring into being the bound-state, oscillation-state, and bi-oscillation-state solitary waves, as described in Figs. 8 and 9. For the interaction between the two modulated solitary waves, bound-state, oscillation-state, and bi-oscillation-state solitary waves with short-time variations of shapes or appearances of the bulges have been observed, as seen in Figs. 10–12. Due to the modulations of the long waves, breathers and rogue waves have been distorted and stretched in the evolution, as shown in Figs. 13 and 14. Those distortions and
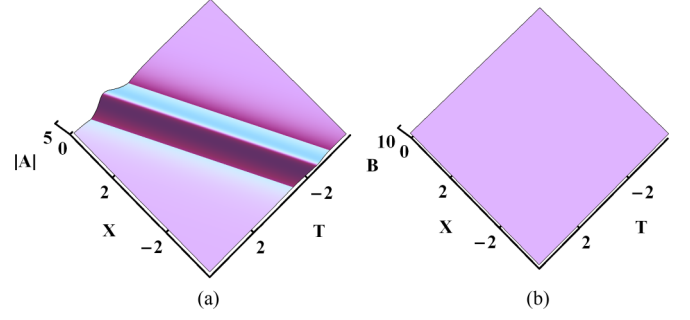
stretches have been seen to be mainly manifested in two aspects: one is the evolution trajectories for the breathers; the other is the shape variations for each element of the breathers as well as the rogue waves. Numbers of peaks and valleys for the rogue waves have been demonstrated to be adjustable via the modulations. In addition, we have found that the modulated breathers and rogue waves can degenerate into the M- or W-shaped or multipeak solitary waves under certain conditions, as presented in Figs. 15 and 16.

APPENDIX A

The $|g_1 + g_3|^2$ and $|1 + f_2 + f_4|^2$ are presented as

$$
|g_1 + g_3|^2 = e^{2H} + e^{2G} + 2\cos\theta\, e^{H+G} + \frac{P(h_1 a_2^2 + h_2 a_1^2)}{4a_1^2 a_2^2 s_1^2 (C_{g1} - C_{g2})^2} e^{2H+2G} + \frac{P(h_1\cos\theta + q_1\sin\theta)}{4a_1^2 s_1^2 (C_{g1} - C_{g2})^2} e^{3H+G}
$$

$$
+ \frac{P(h_2\cos\theta - q_2\sin\theta)}{4a_2^2 s_1^2 (C_{g1} - C_{g2})^2} e^{H+3G} + \frac{P^2[(q_1 q_2 + h_1 h_2)\cos\theta + (q_1 h_2 - q_2 h_1)\sin\theta]}{32 a_1^2 a_2^2 s_1^4 (C_{g1} - C_{g2})^4} e^{3H+3G}
$$

$$
+ \frac{P^2(q_1^2 + h_1^2)}{64 a_1^4 s_1^4 (C_{g1} - C_{g2})^4} e^{4H+2G} + \frac{P^2(q_2^2 + h_2^2)}{64 a_2^4 s_1^4 (C_{g1} - C_{g2})^4} e^{2H+4G},
$$

$$
|1 + f_2 + f_4|^2 = 1 + \frac{Pe^{2H}}{4a_1^2 (C_{g1} - C_{g2})^2} + \frac{Pe^{2G}}{4a_2^2 (C_{g1} - C_{g2})^2} + \frac{2rPe^{H+G}}{s_1^2 (C_{g1} - C_{g2})^2}
$$

$$
+ \frac{P^2 e^{4H}}{64 a_1^4 (C_{g1} - C_{g2})^4} + \frac{P^2 e^{4G}}{64 a_2^4 (C_{g1} - C_{g2})^4} + \frac{rP^2 e^{3H+G}}{4a_1^2 s_1^2 (C_{g1} - C_{g2})^4} + \frac{rP^2 e^{H+3G}}{4a_2^2 s_1^2 (C_{g1} - C_{g2})^4} + \frac{r^2 P^2 e^{2H+2G}}{s_1^4 (C_{g1} - C_{g2})^4}
$$

$$
+ \frac{(s_1^2 + s_2^2)P^2 e^{2H+2G}}{32 a_1^2 a_2^2 s_1^2 (C_{g1} - C_{g2})^4} + \frac{rs_2^2 P^3 e^{3H+3G}}{32 a_1^2 a_2^2 s_1^4 (C_{g1} - C_{g2})^6} + \frac{s_2^2 P^3 e^{4H+2G}}{256 a_1^4 a_2^2 s_1^2 (C_{g1} - C_{g2})^6} + \frac{s_2^2 P^3 e^{2H+4G}}{256 a_1^2 a_2^4 s_1^2 (C_{g1} - C_{g2})^6}
$$

$$
+ \frac{s_2^4 P^4 e^{4H+4G}}{4096 a_1^4 a_2^4 s_1^4 (C_{g1} - C_{g2})^8},
$$

with

$$s_1 = (a_1 + a_2)^2 + (b_1 - b_2)^2, \quad s_2 = (a_1 - a_2)^2 + (b_1 - b_2)^2,$$

$$q_1 = 4a_1(b_1 - b_2)\big[a_1^2 - a_2^2 - (b_1 - b_2)^2\big], \quad q_2 = 4a_2(b_1 - b_2)\big[a_1^2 - a_2^2 + (b_1 - b_2)^2\big],$$

$$h_1 = \big[a_2^2 - a_1^2 + (b_1 - b_2)^2\big]^2 - 4a_1^2(b_1 - b_2)^2, \quad h_2 = \big[a_1^2 - a_2^2 + (b_1 - b_2)^2\big]^2 - 4a_2^2(b_1 - b_2)^2,$$

$$r = \cos\theta[(a_1 + a_2)^2 - (b_1 - b_2)^2] + 2\sin\theta(a_1 + a_2)(b_1 - b_2),$$

$$H = c_1 - \frac{a_1 M}{a_1^2 + b_1^2} + a_1 X\left[1 - \frac{\sigma^2}{(a_1^2 + b_1^2)(C_{g1} - C_{g2})^2}\right] - a_1 T\left[C_{g1} - \frac{\sigma^2 C_{g2}}{(a_1^2 + b_1^2)(C_{g1} - C_{g2})^2}\right],$$

$$G = c_2 - \frac{a_2 M}{a_2^2 + b_2^2} + a_2 X\left[1 - \frac{\sigma^2}{(a_2^2 + b_2^2)(C_{g1} - C_{g2})^2}\right] - a_2 T\left[C_{g1} - \frac{\sigma^2 C_{g2}}{(a_2^2 + b_2^2)(C_{g1} - C_{g2})^2}\right],$$

$$\theta = d_1 - d_2 + \frac{M b_1}{a_1^2 + b_1^2} - \frac{M b_2}{a_2^2 + b_2^2} + X\left[b_1 - b_2 + \frac{\sigma^2 b_1}{(a_1^2 + b_1^2)(C_{g1} - C_{g2})^2} - \frac{\sigma^2 b_2}{(a_2^2 + b_2^2)(C_{g1} - C_{g2})^2}\right]$$

$$- T\left[(b_1 - b_2)C_{g1} + \frac{\sigma^2 b_1 C_{g2}}{(a_1^2 + b_1^2)(C_{g1} - C_{g2})^2} - \frac{\sigma^2 b_2 C_{g2}}{(a_2^2 + b_2^2)(C_{g1} - C_{g2})^2}\right].$$

APPENDIX B

The ϖ, p, ϑ_1, ϑ_2, $R(\tau)$, and $W(\tau)$ are expressed as

$$\varpi = \lambda^2\varsigma, \quad R(\tau) = -\frac{1}{Q}\int[\delta - \alpha(\tau)]d\tau, \quad \vartheta_1 = \frac{K^2 + \lambda^2\varsigma \pm \sqrt{K^2(K^2 + 2\lambda^2\varsigma)}}{\lambda^2\varsigma},$$

$$\vartheta_2 = \frac{K^{*2} + \lambda^2\varsigma \mp \sqrt{K^{*2}(K^{*2} + 2\lambda^2\varsigma)}}{\lambda^2\varsigma}, \quad W(\tau) = \frac{-QK \mp i\sqrt{K^2(K^2 + 2\lambda^2\varsigma)}}{Q^2 + K^2 + 2\lambda^2\varsigma}R(\tau),$$

$$p = -\frac{2(K - K^*)^2 + \lambda^2\varsigma[2 - (\vartheta_1\vartheta_1^* + \vartheta_2\vartheta_2^*)]}{2(K + K^*)^2 + \lambda^2\varsigma[2 - (\vartheta_1\vartheta_2 + \vartheta_1^*\vartheta_2^*)]}.$$

[1] J. Pedlosky, J. Atmos. Sci. **27**, 15 (1970).

[2] J. Pedlosky, J. Atmos. Sci. **29**, 680 (1972).

[3] J. D. Gibbon, I. N. James, and I. M. Moroz, Proc. R. Soc. A **367**, 219 (1979).

[4] A. Ludu and J. P. Draayer, Phys. Rev. Lett. **80**, 2125 (1998).

[5] A. Ludu and A. Raghavendra, Appl. Num. Math. **141**, 167 (2019).

[6] A. Ludu, *Nonlinear Waves and Solitons on Contours and Closed Surfaces* (Springer-Verlag, New York, 2012).

[7] A. Ludu and J. P. Draayer, Physica D (Amsterdam) **123**, 82 (1998).

[8] J. E. Hart, Geophys. Fluid Dyn. **3**, 181 (1972).

[9] R. Hide, Phil. Trans. R. Soc. A **250**, 441 (1958).

[10] L. Liu, B. Tian, H. P. Chai, and Y. Q. Yuan, Phys. Rev. E **95**, 032202 (2017); X. Y. Gao, Appl. Math. Lett. **73**, 143 (2017); **91**, 165 (2019).

[11] G. F. Yu, Z. W. Xu, J. Hu, and H. Q. Zhao, Commun. Nonlinear Sci. Numer. Simul. **47**, 178 (2017).

[12] X. Y. Xie, B. Tian, L. Liu, X. Y. Wu, and Y. Jiang, Mod. Phys. Lett. B **30**, 1650412 (2016); X. H. Zhao, B. Tian, X. Y. Xie, X. Y. Wu, Y. Sun, and Y. J. Guo, Wave Random Complex Media **28**, 356 (2018); Y. Q. Yuan, B. Tian, L. Liu, X. Y. Wu, and Y. Sun, J. Math. Anal. Appl. **460**, 476 (2018).

[13] R. Guo and Y. F. Liu, Appl. Math. Comput. **259**, 153 (2015).

[14] R. Guo, H. Q. Hao, and L. L. Zhang, Nonlinear Dyn. **74**, 701 (2013); H. M. Yin, B. Tian, J. Chai, and X. Y. Wu, Appl. Math. Lett. **82**, 126 (2018); Z. Du, B. Tian, H. P. Chai, and Y. Q. Yuan, Commun. Nonlinear Sci. Numer. Simulat. **67**, 49 (2019).

[15] X. Y. Wen and Z. Yan, Chaos **25**, 123115 (2015).

[16] G. Zhang, Z. Yan, and X. Y. Wen, Chaos **27**, 083110 (2017).

[17] X. Wang, Y. Li, F. Huang, and Y. Chen, Commun. Nonlinear Sci. Numer. Simulat. **20**, 434 (2015).

[18] A. M. Kamchatnov and M. V. Pavlov, J. Phys. A **28**, 3279 (1995).

[19] B. Tan and J. P. Boyd, Stud. Appl. Math. **109**, 67 (2002).

[20] L. Wang, Z. Q. Wang, J. H. Zhang, F. H. Qi, and M. Li, Nonlinear Dyn. **86**, 185 (2016).

[21] L. Wang, Z. Z. Wang, D. Y. Jiang, F. H. Qi, and R. Guo, Eur. Phys. J. Plus **130**, 199 (2015).

[22] V. E. Zakharov and A. B. Shabat, Funct. Anal. Appl. **8**, 226 (1974).

[23] C. S. Gardner, J. M. Greene, M. D. Kruskal, and A. R. M. Miura, Phys. Rev. Lett. **19**, 1095 (1967).

[24] R. Hirota, *The Direct Method in Soliton Theory* (Springer-Verlag, Berlin, 1980).

[25] B. L. Guo, L. M. Ling, and Q. P. Liu, Phys. Rev. E **85**, 026607 (2012).

[26] M. Sato, North-Holland Mathematics Studies **81**, 259 (1983).

[27] W. R. Sun and L. Wang, Proc. R. Soc. A **474**, 20170276 (2018).

[28] A. Hasegawa and F. Tappert, Appl. Phys. Lett. **23**, 142 (1973).

[29] E. A. Kuznetsov and F. Dias, Phys. Rep. **507**, 43 (2011).

[30] J. Zabusky and C. J. Galvin, J. Fluid Mech. **47**, 811 (1971).

[31] W. R. Sun, D. Y. Liu, and X. Y. Xie, Chaos **27**, 043114 (2017).

[32] L. Wang, J. H. Zhang, C. Liu, M. Li, and F. H. Qi, Phys. Rev. E **93**, 062217 (2016).

[33] D. S. Wang, S. W. Song, B. Xiong, and W. M. Liu, Phys. Rev. A **84**, 053607 (2011); C. R. Zhang, B. Tian, L. Liu, H. P. Chai, and Z. Du, Wave Motion **84**, 68 (2019); X. X. Du, B. Tian, X. Y. Wu, H. M. Yin, and C. R. Zhang, Eur. Phys. J. Plus **133**, 378 (2018); C. C. Hu, B. Tian, X. Y. Wu, Y. Q. Yuan, and Z. Du, ibid. **133**, 40 (2018).

[34] L. Liu, B. Tian, Y. Q. Yuan, and Z. Du, Phys. Rev. E **97**, 052217 (2018); S. S. Chen, B. Tian, L. Liu, Y. Q. Yuan, and C. R. Zhang, Chaos, Solitons Fractals **118**, 337 (2019).

[35] T. Xu, M. Li, and L. Li, Europhys. Lett. **109**, 30006 (2015). H. M. Yin, B. Tian, J. Chai, L. Liu, and Y. Sun, Comput. Math. Appl. **76**, 1827 (2018); Z. Du, B. Tian, H. P. Chai, Y. Sun, and X. H. Zhao, Chaos Solitons Fractals **109**, 90 (2018).

[36] Z. Y. Yan, Phys. Lett. A **375**, 4274 (2011).

[37] E. Pelinovsky and C. Kharif, *Extreme Ocean Waves* (Springer-Verlag, Berlin, 2008).

[38] A. R. Osborne, *Nonlinear Ocean Waves and the Inverse Scattering Transform* (Elsevier, New York, 2010).

[39] N. Akhmediev, J. M. Soto-Crespo, and A. Ankiewicz, Phys. Lett. A **373**, 2137 (2009).

[40] L. Wang, J. H. Zhang, Z. Q. Wang, C. Liu, M. Li, F. H. Qi, and R. Guo, Phys. Rev. E **93**, 012214 (2016).

[41] C. Q. Dai, G. Q. Zhou, and J. F. Zhang, Phys. Rev. E **85**, 016603 (2012).

[42] H. Q. Zhang, Y. Wang, and W. X. Ma, Chaos **27**, 073102 (2017).

[43] D. S. Wang, X. H. Hu, and W. M. Liu, Phys. Rev. A **82**, 023612 (2010).

[44] W. X. Ma, T. W. Huang, and Y. Zhang, Phys. Scr. **82**, 065003 (2010).

[45] H. Q. Zhang, B. Tian, X. H. Meng, X. Lü, and W. J. Liu, Eur. Phys. J. B **72**, 233 (2009).

[46] P. Rhines, Geophys. Fluid Dyn. **1**, 273 (1970).

[47] S. J. Miller, O. H. Shemdin, and M. S. Longuet-Higgins, J. Fluid Mech. **233**, 389 (1991).

[48] L. C. Zhao, S. C. Li, and L. M. Ling, Phys. Rev. E **93**, 032215 (2016); M. L. Ren, J. S. Berger, W. J. Liu, G. R. Liu, and R. Agarwal, Nat. Commun. **9**, 186 (2018).